Published in final edited form as:
Chem Senses. 2006 March ; 31(3): 197–206.

Pulse Stimulation with Odors or IBMX/Forskolin Potentiates Responses in Isolated Olfactory Neurons

Wenling Zhang and **Rona J. Delay**
Department of Biology, University of Vermont, Burlington, VT 05405, USA

Abstract

Many odor responses are mediated by the adenosine 3′,5′-cyclic monophosphate (cAMP) pathway in which the cAMP-gated current is amplified by Ca^{2+}-dependent Cl^- current. In olfactory neurons, prolonged exposure to odors decreases the odor response and is an adaptive effect. Several studies suggest that odor adaptation is linked to elevated intracellular Ca^{2+}. In the present study, using the perforated configuration of the patch clamp technique, we found that repetitive odor stimulation elicits a potentiation of the subsequent responses in olfactory neurons. This potentiation is mimicked by stimulating the cAMP pathway and does not appear to be related to phosphorylation of ion channels since protein kinase inhibitors could not block it. Our data suggest that local increases in $[Ca^{2+}]_i$ via activation of the cAMP pathway mediate the pulse-elicited potentiation. In the first odor application, entry of Ca^{2+} through cyclic nucleotide–gated channels appears to be buffered. Repetitive stimulation allows local increases in $[Ca^{2+}]_i$, recruiting more Ca^{2+}-dependent Cl^- channels with each subsequent odor pulse.

Keywords

chloride channel; CNG channel; mudpuppy

Introduction

All cells respond to chemicals in their external environment. In complex organisms, one of the most important chemical sensing systems is olfaction, which plays a significant role in animal behaviors such as feeding, territorial recognition, and social activity. Odorants bind to receptor proteins located on the cilia of the olfactory sensory neuron (OSN) and trigger the production of intracellular chemical signals. These second messengers directly or indirectly target ion channels, resulting in a flux of ions across the ciliary membranes. There are several second-messenger pathways that can be involved in odor transduction: adenosine 3′,5′-cyclic monophosphate (cAMP), inositol 1,4,5-trisphosphate, nitric oxide, carbon monoxide, and 3-phosphoinositide–mediated pathways (Boekhoff et al., 1990; Fadool and Ache, 1992; Lischka and Schild, 1993; Leinders-Zufall et al., 1995; Schild and Restrepo, 1998; Spehr et al., 2002). In rodents, studies have shown that odor activation of G_{olf}, a G protein that is coupled with olfactory response, stimulates adenylyl cyclase III, resulting in increased cAMP, that directly activates nonselective cation channels (Leinders-Zufall et al., 1997; Dzeja et al., 1999). Ca^{2+} influx through cyclic nucleotide–gated channels (CNG channels) activates Ca^{2+}-dependent Cl^- conductance, which can further depolarize the OSN (Kleene and Gesteland, 1991; Kleene, 1993; Kurahashi and Yau, 1993). In many of the second-messenger pathways that may mediate odor transduction, Ca^{2+} ions play either a central or a peripheral role.

Correspondence to be sent to: Rona J. Delay, 104 Marsh Life Science Building, Department of Biology, University of Vermont, Burlington, VT 05405, USA. e-mail: rona.delay@uvm.edu.

Since Ca^{2+} ions are a fundamental signaling component in cells, regulating a diverse variety of cellular functions, free intracellular Ca^{2+}, $[Ca^{2+}]_i$, is tightly regulated. Not only are there multiple mechanisms for Ca^{2+} removal (Na/Ca exchangers, Ca adenosine triphosphatases, Ca ion pumps) but many cellular components, notably, smooth endoplasmic reticulum and mitochondria, remove free Ca^{2+} ions by sequestering it. In the cytosol, Ca-binding proteins (CBPs) abound. Many of these CBPs have been found in olfactory neurons including hippocalcin, calmodulin (CaM), p26olf, neurocalcin, calretinin, and neuron-specific calcium sensor 1 (Bastianelli et al., 1995; Malz et al., 2000; Miwa et al., 2001; Mammen et al., 2004; Treloar et al., 2005). CBPs can serve in calcium transport as Ca regulators or as activator proteins.

Odor perception not only relies on the chemical structure of an odorant and the extent of stimulation but also on the functional state of the OSNs. Exposure of the olfactory system to an odorant can inhibit or enhance the odorant sensitivity (Wang et al., 1993; Zufall and Leinders-Zufall, 2000). Prolonged exposure to odors leads to a decrease in odor response in olfactory neurons and is a type of adaptation. At the cellular level, Leinders-Zufall et al. (1998) showed that odor adaptation occurs in the olfactory cilia. They found that in isolated salamander OSNs, a second odor stimulation evokes less response than the odor response evoked by the first stimulation. Similar results have been observed in both salamander and newt (Kurahashi and Shibuya, 1990; Kurahashi and Menini, 1997; Leinders-Zufall et al., 1999). This short-term adaptation is related to the dynamics of the Ca^{2+} signal. So far two mechanisms of short-term adaptation have been reported.

The first mechanism occurs when the increase of intracellular Ca^{2+} blocks CNG channels (Zufall et al., 1991) via a Ca^{2+}-dependent protein that inhibits the binding of cAMP to the CNG channel (Kramer and Siegelbaum, 1992). Since olfactory CNG channels are composed of three subunits: CNGA2, CNGA4, and CNGB1b, one accepted hypothesis is that Ca^{2+}/CaM binds to the subunit CNGA2 that inhibits the channel and leads to adaptation (Trudeau and Zagotta, 2003). However, Bradley et al. (2004) found that the native subunits CNGA4 and CNGB1b can also associate with CaM to inhibit these channels in the presence of Ca^{2+}.

The second mechanism is dependent on Ca^{2+}/calmodulin kinase II (CaMKII). Elevation of Ca^{2+} activates CaMKII, which inhibits the activity of adenylyl cyclase III through a phosphorylation pathway (Wei et al., 1998; Leinders-Zufall et al., 1999).

Besides short-term adaptation, there is also a slower, longer lasting decrease in intensity of odor perception in OSNs termed long-lasting adaptation. In *Caenorhabditis elegans*, long-lasting adaptation takes place within a few hours (Colbert and Bargmann, 1995). In isolated salamander OSNs, a cyclic guanosine monophosphate analog causes a slow and long-lasting (several minutes) elevation of Ca^{2+} through the CNG channels (Leinders-Zufall et al., 1997). Olfactory adaptation is a common phenomenon and has been well studied, especially with behavioral tests.

Increases in odor sensitivity as measured by behavioral responses and electro-olfactogram (EOG) have also been reported (Youngentob and Kent, 1995; Yee and Wysocki, 2001). The increased sensitivity was thought to be due to a change in odor receptor expression in immature OSNs rather than due to changes in mature OSNs, but this remains to be determined.

Here we present evidence that when isolated OSNs are stimulated repetitively with odors the response increases over a few minutes. Pulse stimulation with 3-isobutyl-1-methylxanthine (IBMX) + forskolin, 7-deacetyl-7-[*O*-(*N*-methylpiperazino)-γ-butyryl]-forskolin dihydrochloride (forskolin) (IF), which activates the cAMP pathway directly, mimics this effect. After the initial stimulation-induced Ca^{2+} influx and the presumptive saturation of a

putative endogenous CBP, the potentiation of the repetitive responses appears to be a function of Cl^- amplification.

Materials and Methods

Subjects

Healthy adult mudpuppies (*Necturus maculosus*) of both sexes were obtained from Kons Scientific Co. (Germantown, WI) and maintained in aquaria at 4–8°C. All procedures were conducted under the supervision of University of Vermont Animal Care and Use Committee.

Physiological recordings

Mudpuppy OSNs were dissociated from the sensory epithelium of adult animals using an enzyme-free procedure described by Dionne (1992). Briefly, olfactory sacs were removed from the animal and placed into amphibian physiological saline (APS; see Table 1). The epithelium was removed, cut into pieces, and then placed into a low-calcium dissociation solution containing (in millimolars) 110 NaCl, 4 NaOH, 2 KCl, 1 $CaCl_2$, 10 Na_2CO_3, 10 $NaHCO_3$, 10 $C_6H_6Na_3O_7$, 0.1 albumin, and pH 10.3 for 15 min. The treated tissues were transferred to APS containing 0.5 μg/ml deoxyribonuclease and stirred gently. The dissociated OSNs remained viable for 5 h. The isolated OSNs were plated into a recording chamber and viewed with 40× objectives (400× total) on a Nikon inverted microscope. Patch electrodes of borosilicate glass were pulled on a Flaming/Brown micropipette puller (Sutter Instruments, Novato, CA). The resistance of the micropipette ranged from 3 to 5 MΩ. After a seal of 3–5 GΩ was obtained, the membrane was slowly perforated by gramicidin (0.7 mg/ml in the intracellular solution; see Table 2). Gramicidin is a pore-forming agent that allows Na^+ and K^+ to pass but not Cl^- or Ca^{2+}. All recordings were conducted at room temperature, and the data were collected using a Digidata 1320A, an Axopatch 200B, and Clampex 8.2 software (Axon Instruments, Foster City, CA) with a low-pass Bessel filter set at 1 kHz. A SF-77B perfusion system (Warner Instrument Co., Hamdon, CT) was used to rapidly apply the test solutions including different odorants or drugs. Under patch clamp recording conditions, OSNs remained viable longer if the membrane was held close to the resting potential (approximately −60 mV). Therefore, in order to extend the recording time and still record current responses at different holding potentials, we used three different recording protocols. A one-step protocol stepped the potential to −80 mV for 5 s with a 2-s odor stimulation in the middle of the pulse. The two-step protocol stepped the potential to −80 mV and +80 mV for 5 s with a 2-s odor stimulation at each step. The third 11-step protocol used voltage steps ranging from −100 to 100 mV in 20-mV steps for 4.5-s pulses with the odor stimuli applied for 1.5 s at each step. In many cases, a single OSN was stimulated with all three protocols. Before recording with a different protocol, each cell was allowed to rest for 5 min. The stimuli for the OSNs included IF (0.1 mM IBMX + 30 μM forskolin) Mix A and Mix B. Mix A was a mixture of seven odorants (100 μM each): hedione, geraniol, phenethylalcohol, citralva, citronellal, eugenol, and menthone. Mix B was a mixture of six odorants (100 μM each): lilial, lyral, ethylvanillin, trethylamine, isolvaleric acid, and phenyl ethyl amine. *N*-[2-((*p*-bromocinnamyl)amino) ethyl]-5-isoquinolinesulfonamide·2HCl (H-89); IBMX; bisindolylmaleimide I (BIM); α-cyano-(3,4,5-trihydroxy)cinnamonitrile, tyrphostin A25 (AG82); 2-(4-morpholinyl)-8-phenyl-4*H*-1-benzopyran-4-one (LY294002); KT5823; forskolin; and 1-[*N*,*O*-bis-(5-isoquinolinesulfonyl)-*N*-methyl-L-tyrosyl]-4-phenylpiperazine (KN62) were obtained from Calbiochem (San Diego, CA) and 1,2-*bis*(*o*-aminophenoxy)ethane-*N*,*N*,*N*′,*N*′-tetraacetic acid, 4K (K^+-BAPTA) and 1,2-*bis*(*o*-aminophenoxy)ethane-*N*,*N*,*N*′, *N*′-tetraacetic acid tetra (acetoxymethyl) ester (BAPTA-AM) from Molecular Probes (Eugene, OR). All test solutions were in APS. All other chemicals were obtained from Sigma Chemical Co. (St. Louis, MO).

Data analysis

The data were analyzed with Origin 7, a scientific graphing and analysis software from OriginLab Corporation (Northampton, MA). Data were represented as mean ± SEM. In order to group responses across OSNs in a single experiment, we normalized the inward current. The inward current (I_{in}) was normalized by setting the magnitude of the peak I_{in} from the first recording in APS to 1. The magnitudes of peak I_{in} in the ensuing recordings were calculated as a percent of the first peak I_{in}. Typically OSNs were tested first with the one-step protocol followed by the 2-step protocol. Although the cell was allowed to rest for 5 min to recover to the unstimulated level, the initial I_{in} in the second experiment with dual-step protocol was somewhat larger than the initial I_{in} in the first experiment with the increase in electrical access due to incorporation of more gramicidin pores. However, the increase of the current caused by incorporation of more gramicidin pores was much slower and smaller than the potentiation we reported in this paper since we started to record the odor responses after the cell was well perforated.

Results

Pulse stimulation with odor mixtures potentiated odor responses in OSNs

Odorants activate second-messenger pathways in OSNs, causing a conductance change. Odor-elicited currents potentiated with repetitive stimulation (Figure 1A). The cell in Figure 1A was stimulated with Mix B at different holding potentials from −100 to 100 mV in 20-mV increments. The protocol was run repetitively. For clarity, only the current trace at −100 mV is displayed. The traces in all figures are numbered in the order they were collected. The peak inward current elicited by Mix B increased over the two recording sets. However, the number of responses to the odor mixtures was quite low: only 2 out of 48 cells (2/48) responded to Mix B, while Mix A elicited only 3/36 inward current responses. Therefore, we mimicked cAMP-mediated odor responses by increasing $[cAMP]_i$ with IF. IBMX is a phosphodiesterase inhibitor that prevents the breakdown of cAMP, and forskolin is an adenylyl cyclase activator. IF elicited responses in over 90% of OSNs tested.

Pulse application of IF potentiated the odor responses

Pulse application of IF mimicked the odor-elicited potentiation (Figure 1B,C). The current responses for a single OSN stimulated with IF at different holding potentials from −100 to 100 mV in 20-mV increments are shown in Figure 1B. Only two traces from each recording set are displayed. The top traces show the outward currents elicited by IF at +100 mV, while the bottom traces show the inward currents elicited by IF at −100 mV. The current–voltage relationship for the IF responses over the three recording sets is displayed in Figure 1C. The peak of inward and outward current elicited by IF increased over the three recording sets. The pulse stimulation of IF changed the shape of the current–voltage relationship (Figure 1C). In the first recording set, IF elicited the largest inward current at −60 mV, whereas in the subsequent recording sets, IF elicited the largest inward current at −100 mV. The magnitude of the peak I_{in} at all the negative potentials increased in the subsequent recordings. Similar results were obtained from 72 OSNs with different recording time intervals. We found that if the time interval between repetitive recordings was less than 1 min, the potentiation of inward currents was significant. If the OSNs were unstimulated for 3–5 min, the elicited current returned close to initial value. Therefore, each cell was allowed to rest for 5 min between recording protocols. The outward current elicited by IF also increased with repetitive stimulation but not as significantly as the inward current. Thus, we focused on the changes of the inward current.

Voltage enhancement of the potentiated response

There appeared to be a voltage dependence to the potentiation of the IF response. In order to examine this, we used a single-step (at −80 mV) or two-step (at −80 and +80 mV) protocol as described in Materials and Methods. A typical response pattern at −80 mV with pulse stimulation causing potentiation of the IF-elicited current is displayed in Figure 2A. A single OSN was held at −80 mV for 5 s with IF applied for 2 s. Traces 1, 2, 3, and 4 in Figure 2A were taken at 1-s intervals between recordings. I_{in} elicited by IF increased as the recordings were repeated. After a 5-min recovery, the same OSN in Figure 2A was tested with the two-step protocol. Although only the current traces at −80 mV are displayed in Figure 2B, I_{in} elicited by IF increased significantly with repetitive stimulation. Comparison of the potentiation of the IF response from a single-pulse protocol to a dual-pulse protocol is shown in Figure 2C. The peak I_{in} elicited by IF for OSNs was plotted over time. Since the peak I_{in} varied across the population of OSNs, we normalized I_{in} (see Materials and Methods). The peak I_{in} in the first recording with single-voltage-pulse protocol in APS was set to 1. Over time, the peak I_{in} elicited by IF in the repetitive recordings was increased by using both voltage protocols. The potentiation patterns were similar in 31 cells. Nine OSNs tested with both protocols with the same recording intervals were used to perform statistical analyses. With dual-voltage pulses, I_{in} increased faster and lasted longer than that with a single-voltage step in all the cells tested (n = 9).

Protein kinase inhibitors did not block the potentiation

Since odorants activate second-messenger pathways and might affect ion channels by protein kinase (PK) phosphorylation, different kinase inhibitors were tested to determine whether they blocked the potentiation. The membrane-permeable kinase inhibitors were applied into bath by using the Warner SF-77B perfusion system. A PKA inhibitor (0.2 μM H-89), a PKG inhibitor (0.5 μM KT5823), a CaMKII inhibitor (2 μM KN62), a PKC inhibitor (0.1 μM BIM), a tyrosine kinase inhibitor (20 μM AG82), and a PI3K inhibitor (10 μM LY294002) were tested, but none of them inhibited the IF-caused potentiation (data not shown).

Cl^- flux carried the IF response potentiation

Since previous studies showed that chloride current is an essential element of odor responses (Kleene and Gesteland, 1991; Kleene, 1993), it was important to determine whether Cl^- flux played a role in the potentiation. Niflumic acid (NA), a chloride channel blocker, blocked 90 ± 2% (n = 8) of the control I_{in} in mudpuppy OSNs. NA blocked the potentiation of the IF response under the three-voltage-pulse protocols, shown in Figure 3. Figure 3A shows the two recording traces from a single OSN using the 11-voltage-pulses protocol (as described in Materials and Methods). Both traces occurred at −100 mV. The lower trace is the IF-elicited I_{in} in APS while the upper trace is the IF-elicited I_{in} with 300 μM NA in APS. NA greatly reduced the IF-generated response. The shape of the inward current trace also changed. In APS, with repetitive stimulation of IF, the inward current increased faster, and there was a sustained current in the late phase. With NA in the bath, the inward current peaked more slowly and returned to baseline more quickly. Similar results were obtained from 36 cells. Potentiation with IF pulse stimulation required chloride current, shown in Figure 3B,C. Under the single-voltage-pulse protocol, the peak I_{in} increased over time with repetitive stimulations in APS. In the presence of NA, IF response decreased and the pulse enhancement was blocked (n = 5, Figure 3B). Even the dual-voltage protocol could not recover the pulse stimulation increase of the IF response. Figure 3C showed the normalized IF responses over time as Figure 3B under the dual-voltage-pulse protocol for the same five cells.

Increases in intracellular Ca^{2+} levels played a role in the potentiation of I_{in} elicited by IF

Odorant responses involve entry of Ca^{2+} into the OSNs (Restrepo et al., 1993; Leinders-Zufall et al., 1998). To determine the role of Ca^{2+} in the potentiation of I_{in} elicited by IF, bath Ca^{2+} was replaced by Ba^{2+}. Substitution of Ba^{2+} for Ca^{2+} eliminated most of the potentiation of IF-elicited responses in OSNs (Figure 4). Under the single-voltage-pulse protocol, Ba^{2+} decreased I_{in} elicited by IF and the short-term potentiation was decreased as well (Figure 4A). Similar results were observed with the dual-step protocol with the same cells as in A after a 5-min rest. Even with the dual-voltage-pulse protocol, the pulse stimulation enhancement did not recover (Figure 4B). Under the 11-step voltage protocol, substitution of Ba^{2+} for Ca^{2+} reduced a large part of the IF response in 16 OSNs.

If an influx of Ca^{2+} is required for the pulse potentiation, use of a Ca^{2+} buffer should change the response. Two methods were used to buffer intracellular Ca^{2+}. First, we used BAPTA-AM, a membrane-permeable Ca^{2+} chelator, to buffer the intracellular Ca^{2+} in OSNs. The IF-elicited response as measured with the single-pulse protocol in APS, Ba^{2+}-APS, and BAPTA-AM–Ba^{2+}-APS is shown in Figure 5A ($n = 3$). I_{in} increased with repetitive recordings in APS. In Ba^{2+}-APS, a large portion of the potentiation was eliminated. Inclusion of BAPTA-AM further reduced the potentiation response, which implied that there was still a small amount of Ca^{2+} left in Ba^{2+}-APS. The results implied that the potentiation of the odorant response elicited by IF was related to the entry of Ca^{2+} into the OSNs and the increase of intracellular $[Ca^{2+}]$.

Second, to confirm the BAPTA-AM results, we used whole-cell recordings with 5 mM K^+-BAPTA in the intracellular solution. Approximately 100 s after the membrane was ruptured, the single-pulse protocol was used to stimulate the cell with IF for about 1 min, followed by the dual-pulse protocol. With the single-pulse protocol, I_{in} elicited by IF increased and then leveled out quickly (Figure 5B). Directly after testing with the one-step protocol (no recovery period), the cell was tested with the dual-pulse protocol. The IF-elicited inward current increased initially and then decreased. In this cell, 7 min after establishing a whole-cell recording configuration, the IF response disappeared. Similar results were observed in four cells. A similar type of response was observed with the 11-step voltage protocol recorded in whole-cell mode. I_{in} elicited by IF peaked in the second recording and then started to decrease. Five to eight minutes after establishing a whole cell, IF responses disappeared. Similar results were obtained from 15 OSNs.

Potentiation of the odor response elicited by IF is related to intracellular Cl^- concentration

The intracellular Cl^- concentration is a critical element in odorant responses since the majority of the response is carried by Cl^-. As the electrochemical gradient changes, E_{Cl} shifts. Changing the driving force on Cl^- alters the pulse potentiation of IF (Figure 6). Early experiments have shown that during stimulation with the two-step protocol, the IF-elicited response increased faster and lasted longer than that with the single-step protocol (Figure 2C). Since the IF-elicited current response was outward (Cl^- ions moving into the cell) at +80 mV, the entry of the Cl^- ions into the OSN could reestablish the intracellular Cl^- concentration and increase $[Cl^-]_i$. To test this hypothesis, we substituted some of the bath Cl^- with gluconate to decrease the influx of Cl^- ions at +80 mV. Under the dual-voltage-pulse protocol, the peak I_{in} increased with repetitive recordings in the control solution (APS contains 130 mM Cl^-). With the bath Cl^- concentration decreased to 38 mM, the initial increase of I_{in} did not change significantly, but the late-phase increase of I_{in} was inhibited. Figure 6 shows a representative OSN in low Cl^- bath compared with the control (APS). This suggests that the depolarization voltage pulse (+80 mV) allows the Cl^- ions to enter OSNs, which increases the IF-stimulated enhancement. Similar results were observed in four cells.

Discussion

In this paper, we present data that repetitive application of odors or IF potentiates the current responses. Influx of Ca^{2+} is necessary to elicit the pulse stimulation enhancement since a lack of Ca^{2+} influx or buffering intracellular Ca^{2+} inhibits the potentiation elicited by IF. In *Necturus* OSNs, over 90% of the current responses that odorants generate are carried by Cl^- and a block of the Cl^- channels inhibits the pulse stimulation potentiation. The potentiation of the current response is due to the amplification by Ca^{2+}-dependent Cl^- channels.

For many odors, odor transduction involves activation of G_{olf} that stimulates an adenylyl cyclase. The resulting increase in cAMP directly gates CNG channels allowing Ca^{2+} influx. Ca^{2+} activates a Ca^{2+}-dependent Cl^- conductance, which in some cases further depolarizes the olfactory neuron (Kleene and Gesteland, 1991; Kleene, 1993). Prolonged exposure to odors causes adaptation of odor responses. Leinders-Zufall et al. (1999) showed that odor adaptation is related to CaMKII. In rod cells, increased $[Ca^{2+}]_i$ does not inhibit CNG channels if they have been already phosphorylated by tyrosine kinase (Krajewski et al., 2003). Since phosphorylation can inhibit the adaptation of the response, different kinase inhibitors were tested to determine whether any PKs mediated the IF-elicited potentiation. However, none of the tested PK inhibitors (PKA inhibitor, PKG inhibitor, CaMKII inhibitor, PKC inhibitor, tyrosine kinase inhibitor, PI3K inhibitor) blocked the potentiation. Therefore, this enhanced odorant response elicited by IF did not appear to be related to a change in the phosphorylation of the ion channels which involves odor signal transduction.

Using the whole-cell patch clamp recording technique, Kurahashi and Shibuya (1990) found that prolonged stimulation with odorants decreased the current response gradually over a 9-s application in newt OSNs, and this effect is mediated by Ca^{2+} influx. Recording from an inside-out patch from dendrites and cilia of catfish OSNs, Kramer and Siegelbaum (1992) found that Ca^{2+} inhibits the binding of cAMP to CNG channels by a regulatory protein, which might play a role in olfactory adaptation. Leinders-Zufall et al. (1998) showed that odor adaptation occurs in the olfactory cilia of isolated salamander OSNs and that a second odor stimulation evokes less response than the odor response evoked by the first stimulation using the perforated patch clamp technique with amphotericin B. Our results appear to be in conflict with these published reports. We found that the repetitive stimulation of odorants or IF potentiated the responses, although after several minutes the responses decreased. One possible explanation for this might be due to the difference between the recording techniques used.

Whole-cell recordings can significantly change the intracellular environment, not only of ions (Ca^{2+}, Cl^-) but also of the soluble second messengers. Leinders-Zufall et al. (1998) used the perforated patch clamp technique with amphotericin B, which leaves the intracellular Ca^{2+} unbuffered by exogenous agents. However, amphotericin B pores disturb the native intracellular concentration of Cl^- since chloride ions flow through amphotericin B pores (Khutorsky, 1996; Resat and Baginski, 2002), although more slowly than sodium and potassium. We used the perforated patch clamp technique with gramicidin to record odor responses (except Figure 5B). With gramicidin as the pore-forming agent, only sodium and potassium ions cross the membrane (Hille, 1992). Thus, intracellular Ca^{2+} concentration was not changed, and only endogenous Ca buffers were present. $[Cl^-]_i$ was undisturbed. Since intracellular Cl^- appears to play a major role in the application of the odor responses, any change in $[Cl^-]_i$ would profoundly affect this potentiation. When we used the whole-cell configuration of the patch clamp technique with BAPTA as a Ca^{2+} buffer, and the potentiation was only apparent in the first 3 min, then the response ran down.

It is possible that other variables could make our result different from others. One possibility could be that we used a combination of IF. IF response mimicked the odor response; however,

IF are not odorants. IF evoked much larger responses than the odorant responses we usually recorded. Almost all the OSNs responded to IF, but only a small percentage of the tested OSNs responded to odorants. Therefore, the combination of the two drugs may cause some special effects. However, since odor mixtures evoked a similar potentiation like IF, it seems unlikely (see Figure 1). Another possibility is that the potentiation is species related. However, we also found that repetitive stimulation of IF caused potentiation of the response in mouse OSNs, so this phenomenon is not restricted in one species (unpublished data).

With over 90% of the IF-generated current carried by Cl^- ions, any change in the Cl^- flux would greatly affect the IF response. This suggests that the intracellular Cl^- in *Necturus* olfactory neurons is quite high, similar to intracellular Cl^- concentrations reported in other species, including ~40 mM in newt OSNs, ~81 mM in rat OSNs soma, ~93 mM in mouse OSNs soma, and 40–50 mM in dendritic knobs in rodents OSNs (Nakamura et al., 1997; Kaneko et al., 2001, 2004; Delay et al., 2004). As the electrochemical gradient for Cl^- changes, E_{Cl} shifts. The IF-generated current response is inward at −80 mV and outward at +80 mV; chloride ions flow into the cell during the response at +80 mV. Thus, this influx of Cl^- ions elicited at +80 mV step should increase both the intracellular chloride ion concentration and the driving force on Cl^- with successive stimulations. To test this hypothesis, the bath Cl^- concentration was lowered to decrease the influx of Cl^- ions at +80 mV to determine whether this would affect the potentiation of IF response. Under the dual-voltage-pulse protocol, with the bath Cl^- concentration decreased from 130 mM to 38 mM, the initial increase of I_{in} was unchanged significantly, but the late-phase increase of I_{in} was inhibited. This suggested that Cl^- ions entered OSNs at the +80-mV step, and the resulting increase in $[Cl^-]_i$ was responsible for the IF-stimulated enhancement in the late phase. In low bath chloride, less recharging of intracellular Cl^- occurs.

It has been suggested that olfactory signal transduction takes place in a protein complex in the ciliary membrane. Reisert et al. (2003) proposed that CNG channels and Cl^- channels in the rat OSNs are not tightly clustered in a transduction complex but separated from each other in a regularly spaced matrix. Ca^{2+} entry through CNG channels must diffuse to reach the Cl^- channels. Thus, for a given Cl^- channel, all the surrounding CNG channels would contribute some level of Ca^{2+} for activation, with the nearest CNG channel supplying the greatest contribution of Ca^{2+} for the Cl^- channel. If CNG channels are separated from Cl^- channels, there could be intracellular CBPs located between the channels (Figure 7A). The first entry of Ca^{2+} through a CNG channel elicited by IF would not activate many Cl^- channels since most of the Ca^{2+} would bind to the CBPs. Once the CBPs are fully bound with Ca^{2+}, the intracellular $[Ca^{2+}]$ increases with repetitive stimulation and activates more Ca^{2+}-dependent Cl^- channels, amplifying the response (Figure 7B). With the dual-pulse protocol, stimulation at +80 mV elicits an outward current and Cl^- ions flow into the cell. This influx augments intracellular Cl^-, enhancing the subsequent responses at −80 mV (Figure 7C).

In conclusion, pulse application of odors or IF to mudpuppy OSNs potentiated the odorant response. This potentiation of the odorant response did not appear to be phosphorylation-dependent but rather due to activation of more Ca^{2+}-dependent Cl^- channels from increased Ca^{2+} diffusion from CNG channels.

Acknowledgements

The work was supported by grants R03DC03912, P20RR16435, and DC006939 from the National Institutes of Health.

References

Bastianelli E, Polans AS, Hidaka H, Pochet R. Differential distribution of six calcium-binding proteins in the rat olfactory epithelium during postnatal development and adulthood. J. Comp. Neurol 1995;354:395–409. [PubMed: 7541806]

Boekhoff I, Tareilus E, Strotmann J, Breer H. Rapid activation of alternative second messenger pathways in olfactory cilia from rats by different odorants. EMBO J 1990;9:2453–2458. [PubMed: 2164471]

Bradley J, Bonigk W, Yau KW, Frings S. Calmodulin permanently associates with rat olfactory CNG channels under native conditions. Nat. Neurosci 2004;7:705–710. [PubMed: 15195096]

Colbert HA, Bargmann CI. *Odorant-specific adaptation pathways generate olfactory plasticity in* C. elegans. Neuron 1995;14:803–812. [PubMed: 7718242]

Delay RJ, Verret TJ, Gorman R. Chloride homeostasis in mouse olfactory neurons. Achems. Abstr., Chem. Senses 2004;30:265–278.

Dionne VE. *Chemosensory responses in isolated olfactory receptor neurons from* Necturus maculosus. J. Gen. Physiol 1992;99:415–433. [PubMed: 1588301]

Dzeja C, Hagen V, Kaupp UB, Frings S. Ca2+ permeation in cyclic nucleotide-gated channels. EMBO J 1999;18:131–144. [PubMed: 9878057]

Fadool DA, Ache BW. Plasma membrane inositol 1,4,5-trisphosphate-activated channels mediate signal transduction in lobster olfactory receptor neurons. Neuron 1992;9:907–918. [PubMed: 1384577]

Hille, B. Ionic Channels of Excitable Membranes. Sinauer Associates; Sunderland, MA: 1992.

Kaneko H, Nakamura T, Lindemann B. Noninvasive measurement of chloride concentration in rat olfactory receptor cells with use of a fluorescent dye. Am. J. Physiol. Cell Physiol 2001;280:C1387–C1393. [PubMed: 11350733]

Kaneko H, Putzier I, Frings S, Kaupp UB, Gensch T. Chloride accumulation in mammalian olfactory sensory neurons. J. Neurosci 2004;24:7931–7938. [PubMed: 15356206]

Khutorsky V. Ion coordination in the amphotericin B channel. Biophys. J 1996;71:2984–2995. [PubMed: 8968570]

Kleene SJ. Origin of the chloride current in olfactory transduction. Neuron 1993;11:123–132. [PubMed: 8393322]

Kleene SJ, Gesteland RC. Calcium-activated chloride conductance in frog olfactory cilia. J. Neurosci 1991;11:3624–3629. [PubMed: 1941099]

Krajewski JL, Luetje CW, Kramer RH. Tyrosine phosphorylation of rod cyclic nucleotide-gated channels switches off Ca2+/calmodulin inhibition. J. Neurosci 2003;23:10100–10106. [PubMed: 14602825]

Kramer RH, Siegelbaum SA. Intracellular Ca2+ regulates the sensitivity of cyclic nucleotide-gated channels in olfactory receptor neurons. Neuron 1992;9:897–906. [PubMed: 1384576]

Kurahashi T, Menini A. Mechanism of odorant adaptation in the olfactory receptor cell. Nature 1997;385:725–729. [PubMed: 9034189]

Kurahashi T, Shibuya T. Ca2(+)-dependent adaptive properties in the solitary olfactory receptor cell of the newt. Brain Res 1990;515:261–268. [PubMed: 2113412]

Kurahashi T, Yau KW. Co-existence of cationic and chloride components in odorant-induced current of vertebrate olfactory receptor cells. Nature 1993;363:71–74. [PubMed: 7683113]

Leinders-Zufall T, Greer CA, Shepherd GM, Zufall F. Imaging odor-induced calcium transients in single olfactory cilia: specificity of activation and role in transduction. J. Neurosci 1998;18:5630–5639. [PubMed: 9671654]

Leinders-Zufall T, Ma M, Zufall F. Impaired odor adaptation in olfactory receptor neurons after inhibition of Ca2+/calmodulin kinase II. J. Neurosci 1999;19:1–6. [PubMed: 9870932]RC19

Leinders-Zufall T, Rand MN, Shepherd GM, Greer CA, Zufall F. Calcium entry through cyclic nucleotide-gated channels in individual cilia of olfactory receptor cells: spatiotemporal dynamics. J. Neurosci 1997;17:4136–4148. [PubMed: 9151731]

Leinders-Zufall T, Rosenboom H, Barnstable CJ, Shepherd GM, Zufall F. A calcium-permeable cGMP-activated cation conductance in hippocampal neurons. Neuroreport 1995;6:1761–1765. [PubMed: 8541476]

Lischka FW, Schild D. *Effects of nitric oxide upon olfactory receptor neurones in* Xenopus laevis. Neuroreport 1993;4:582–584. [PubMed: 8390311]

Malz CR, Knabe W, Kuhn HJ. *Pattern of calretinin immunoreactivity in the main olfactory system and the vomeronasal system of the tree shrew,* Tupaia belangeri. J. Comp. Neurol 2000;420:428–436. [PubMed: 10805918]

Mammen A, Simpson PJ, Nighorn A, Imanishi Y, Palczewski K, Ronnett GV, Moon C. Hippocalcin in the olfactory epithelium: a mediator of second messenger signaling. Biochem. Biophys. Res. Commun 2004;322:1131–1139. [PubMed: 15336960]

Miwa N, Shinmyo Y, Kawamura S. Calcium-binding by p26olf, an S100-like protein in the frog olfactory epithelium. Eur. J. Biochem 2001;268:6029–6036. [PubMed: 11732996]

Nakamura T, Kaneko H, Nishida N. Direct measurement of the chloride concentration in newt olfactory receptors with the fluorescent probe. Neurosci. Lett 1997;237:5–8. [PubMed: 9406866]

Reisert J, Bauer PJ, Yau KW, Frings S. The Ca-activated Cl channel and its control in rat olfactory receptor neurons. J. Gen. Physiol 2003;122:349–363. [PubMed: 12939394]

Resat H, Baginski M. Ion passage pathways and thermodynamics of the amphotericin B membrane channel. Eur. Biophys. J 2002;31:294–305. [PubMed: 12122476]

Restrepo D, Okada Y, Teeter JH. Odorant-regulated Ca2+ gradients in rat olfactory neurons. J. Gen. Physiol 1993;102:907–924. [PubMed: 8301263]

Schild D, Restrepo D. Transduction mechanisms in vertebrate olfactory receptor cells. Physiol. Rev 1998;78:429–466. [PubMed: 9562035]

Spehr M, Wetzel CH, Hatt H, Ache BW. 3-phosphoinosi-tides modulate cyclic nucleotide signaling in olfactory receptor neurons. Neuron 2002;33:731–739. [PubMed: 11879650]

Treloar HB, Uboha U, Jeromin A, Greer CA. Expression of the neuronal calcium sensor protein NCS-1 in the developing mouse olfactory pathway. J. Comp. Neurol 2005;482:201–216. [PubMed: 15611992]

Trudeau MC, Zagotta WN. Calcium/calmodulin modulation of olfactory and rod cyclic nucleotide-gated ion channels. J. Biol. Chem 2003;278:18705–18708. [PubMed: 12626507]

Wang HW, Wysocki CJ, Gold GH. Induction of olfactory receptor sensitivity in mice. Science 1993;260:998–1000. [PubMed: 8493539]

Wei J, Zhao AZ, Chan GC, Baker LP, Impey S, Beavo JA, Storm DR. Phosphorylation and inhibition of olfactory adenylyl cyclase by CaM kinase II in neurons: a mechanism for attenuation of olfactory signals. Neuron 1998;21:495–504. [PubMed: 9768837]

Yee KK, Wysocki CJ. Odorant exposure increases olfactory sensitivity: olfactory epithelium is implicated. Physiol. Behav 2001;72:705–711. [PubMed: 11337002]

Youngentob SL, Kent PF. Enhancement of odorant-induced mucosal activity patterns in rats trained on an odorant identification task. Brain Res 1995;670:82–88. [PubMed: 7719728]

Zufall F, Leinders-Zufall T. The cellular and molecular basis of odor adaptation. Chem. Senses 2000;25:473–481. [PubMed: 10944513]

Zufall F, Shepherd GM, Firestein S. Inhibition of the olfac-tory cyclic nucleotide gated ion channel by intracellular calcium. Proc. R. Soc. Lond. B Biol. Sci 1991;246:225–230.

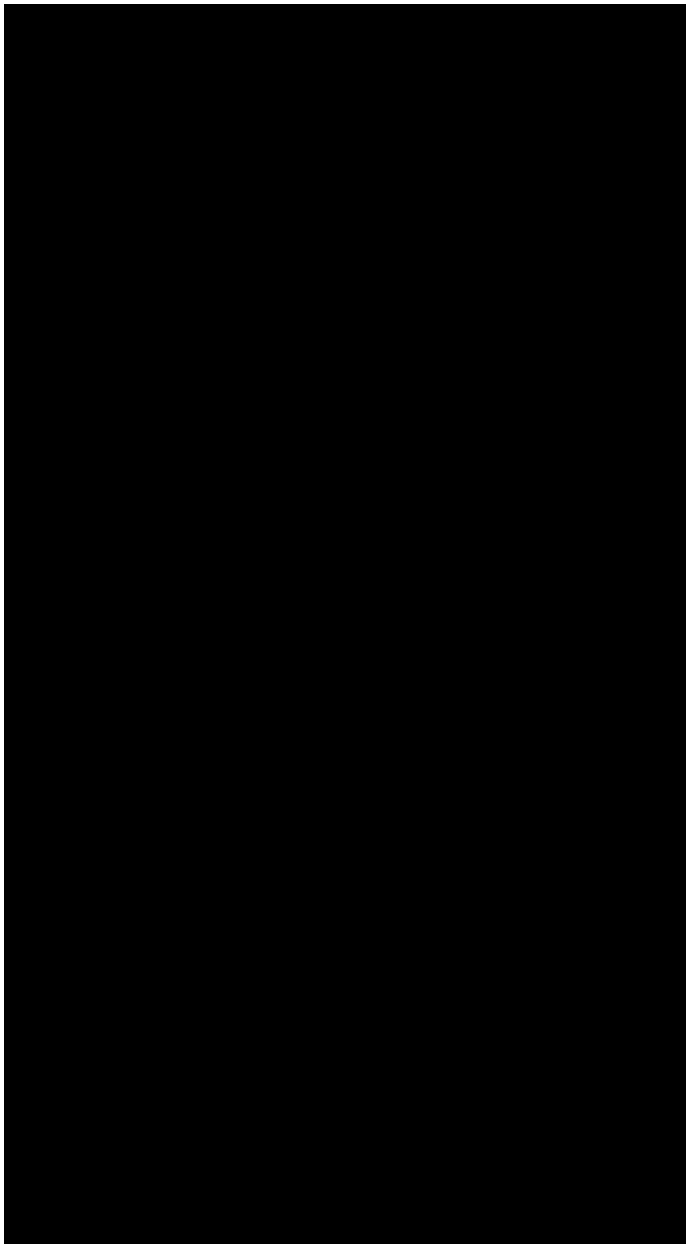

Figure 1.

Pulse stimulation of OSNs with Mix B or IF. **(A)** Pulse stimulation with an odor mixture increased the response. The membrane current was recorded from a single OSN at different voltages from −100 mV to +100 mV in 20-mV increments. Each voltage step lasted for 4.5 s, and Mix B was applied to the OSN for 1.5 s. There was a 20-s interval between the two recordings. Only the current trace recorded at −100 mV is shown. The black bar above the trace represents the application time of Mix B. The traces of the two repetitive recordings are numbered in the order in which they were collected. **(B)** Pulsed increases of $[cAMP]_i$ mimicked the odor-elicited potentiation. The membrane currents were recorded from the OSN using the 11-step protocol. In this and all subsequent figures, the black bar above the trace represents the stimulation time of IF. The top traces show the outward currents elicited by IF at +100 mV, while the bottom traces show the inward currents elicited by IF at −100 mV. The first recording of the OSN is marked 1, and the subsequent recordings are numbered in order collected. There

was a 1-s interval between the recordings. The inward and outward current elicited by IF increased with repetitive stimulation. The magnitude of inward current or outward current was measured as the current from the peak to the baseline (dashed line). **(C)** The pulse stimulation of IF changed the shape of the current–voltage relationship. Pulse stimulation with IF-potentiated current response was largest at more negative potentials. The peak inward and outward current elicited by IF was plotted at each voltage. In the first recording set (Recording 1), IF elicited the largest inward current at −60 mV. In the subsequent recordings, IF elicited the largest inward current at −100 mV. The magnitude of the IF response increased at the more negative and more positive potentials with each repeat.

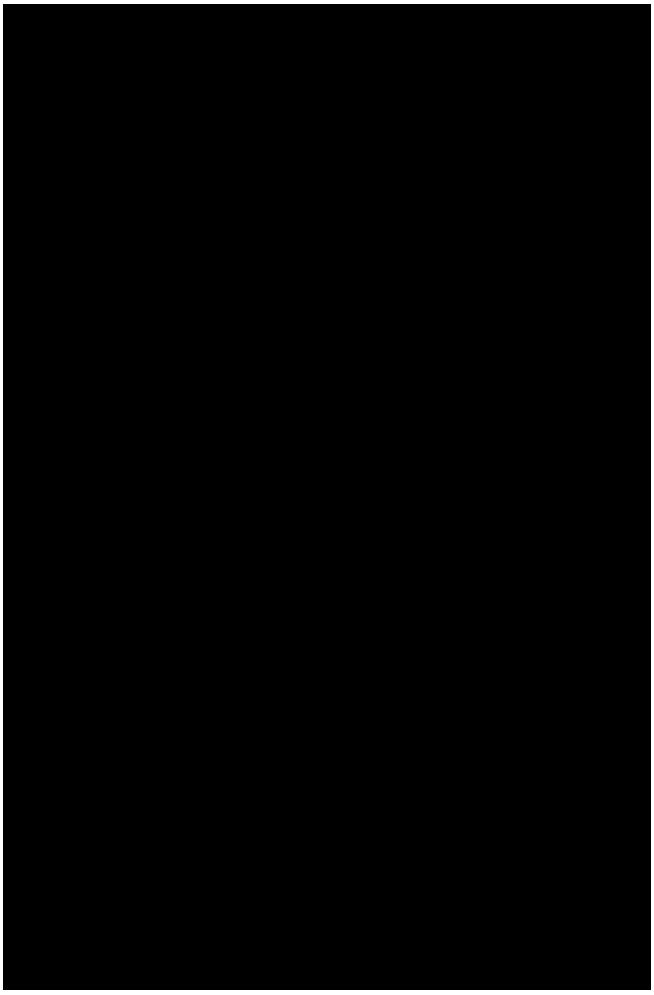

Figure 2.

The increase in IF response was apparent with a single-voltage step and enhanced with a two-step protocol. **(A)** Pulse stimulation at −80 mV elicited a potentiation of the IF-elicited current. At −80 mV, repetitive stimulation increased the IF response. First recording (1) and other traces are numbered in the order collected. Each recording lasted 5 s, and there was a 1-s interval between them. **(B)** After a 5-min rest, the same OSN in (A) was stimulated with dual-voltage pulses, −80 and +80 mV. Only the −80mV current trace is displayed. 1, 2, 3, and 4 are the repetitive recordings numbered in the order collected. There was a 1-s interval between recordings. **(C)** Comparison of the potentiation of IF response from a single-pulse protocol to a dual-pulse protocol. To pool IF responses, the first I_{in} peak for each OSN was set to 1. I_{in} values in other recordings were calculated as fractions of the first I_{in} peak. The IF response was larger and increased faster and longer with the dual-voltage-pulse protocol (n = 9).

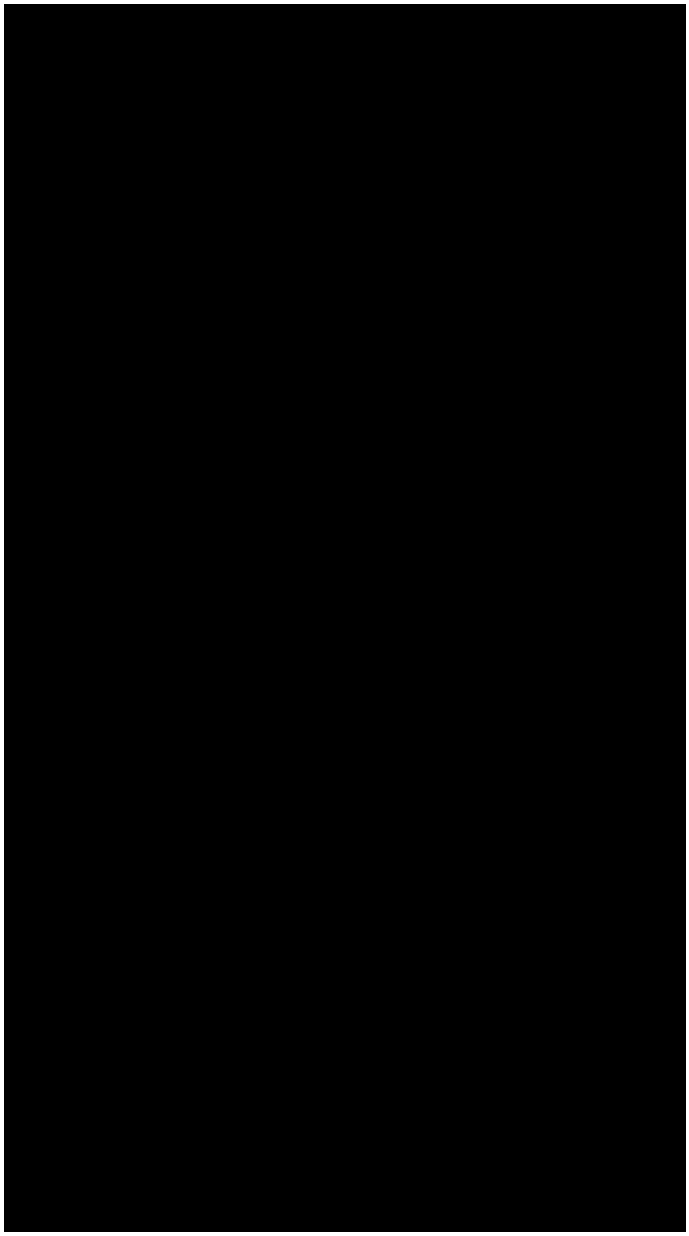

Figure 3.

Cl^- ions carried the majority of the IF-elicited response. **(A)** NA (300 μM), a chloride channel blocker, in the APS was used to block Cl^- channels. A single OSN was stimulated by IF with a 11-step protocol. Only the current trace at −100 mV is shown. The cell was tested in APS first, then with NA, and washed back with APS. The IF response recovered with wash (not shown). **(B)** NA blocked the potentiation of the IF response under the single-voltage-pulse protocol. The peak I_{in} increased with repetitive recordings in APS (solid circle). In the presence of NA, the majority of the I_{in} values elicited by IF disappeared, and the increase of I_{in} was blocked (open circle) (n = 5). **(C)** Dual-step protocol with NA did not restore IF potentiation with the same cells as B after a 5-min rest (n = 5).

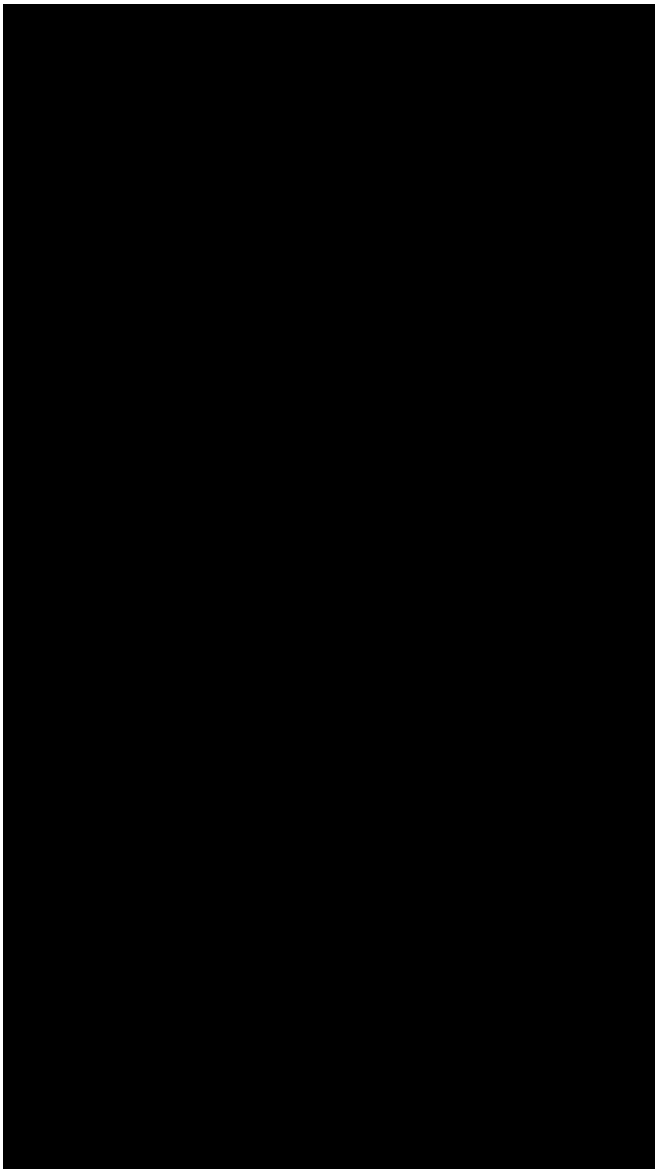

Figure 4.

Substitution of Ba^{2+} for Ca^{2+} eliminated most of the enhancement of I_{in} elicited by IF in OSNs. **(A)** Under the single-voltage-pulse protocol, the peak of I_{in} increased with repetitive recordings in APS (solid circle). When Ca^{2+} in the bath was replaced by Ba^{2+}, majority of I_{in} elicited by IF disappeared and the increase of I_{in} was decreased (open circle) (n = 5). **(B)** Similar results were observed with the dual-step protocol with same cells as A after a 5-min rest (n = 5).

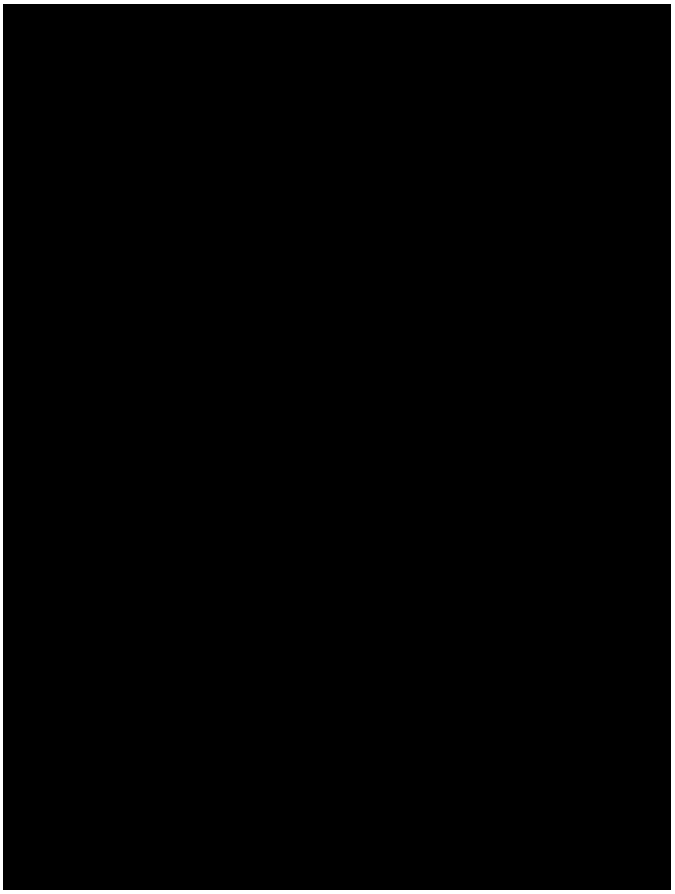

Figure 5.
Ca^{2+} chelators decreased the enhancement of I_{in} elicited by IF in OSNs. **(A)** The IF-elicited response as measured with the single-pulse protocol in APS, Ba^{2+}-APS, and BAPTA-AM–Ba^{2+}-APS. I_{in} increased with repetitive recordings in APS (solid circle). In Ba^{2+}-APS, a large portion of the potentiation was eliminated. Inclusion of a membrane-permeable Ca^{2+} chelator, BAPTA-AM, further reduced the potentiation response ($n = 3$). **(B)** Using whole-cell recording with K^{+}-BAPTA, adenosine triphosphatase, and guanosine triphosphate after the membrane was ruptured, a single OSN was stimulated with IF first by single-pulse protocol (solid circle) and then by dual-pulse protocol (open circle). Similar results were observed in four other cells.

Figure 6.
Changing the driving force on Cl^- altered the pulse potentiation of IF responses. Under the dual-voltage-pulse protocol, the peak of I_{in} increased with repetitive recordings in APS (solid circle) (130 mM Cl^-). When the bath Cl^- concentration was decreased to 38 mM, the late phase of increase of I_{in} was inhibited (open circle).

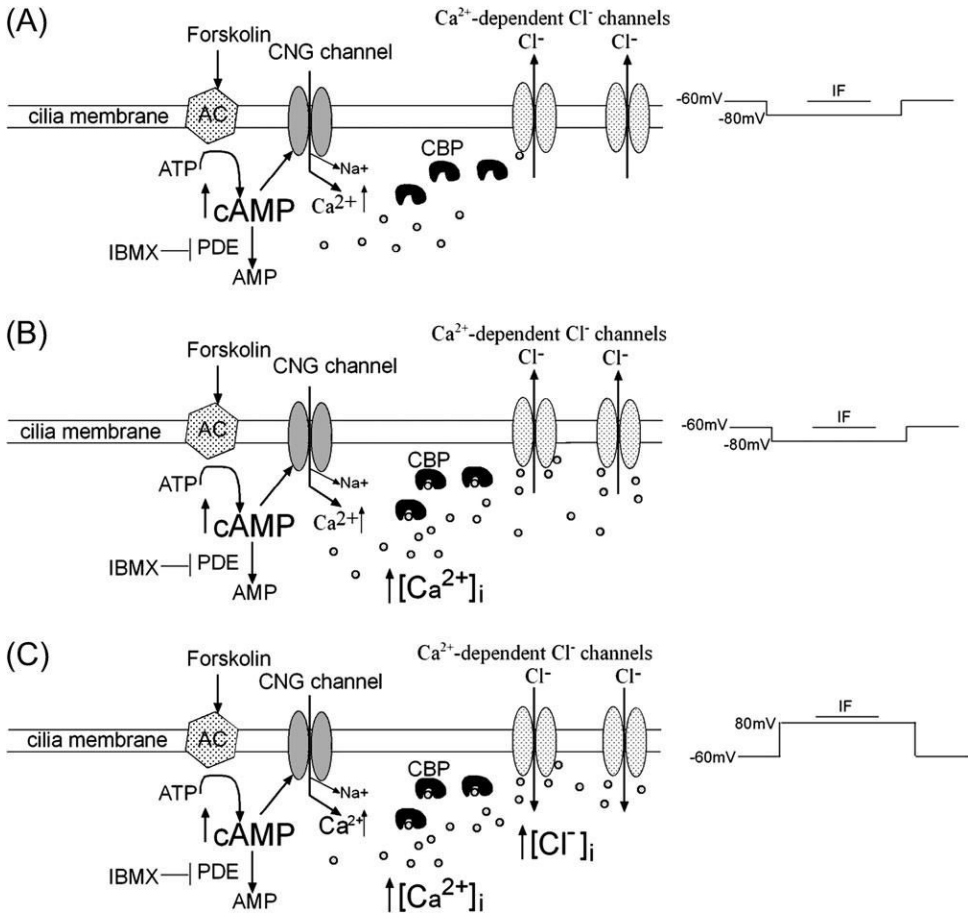

Figure 7.

Possible mechanism for the potentiation of I_{in} elicited by IF. CNG channel, adenylyl cyclase (AC); small circles are Ca^{2+} ions.

Table 1

Bath solutions (in millimolars)

	NaCl	HEPES	KCl	$CaCl_2$	$BaCl_2$	Glucose	Na-gluconate	BAPTA-AM
APS	112	3	2	8		5		
Low Cl APS	20	3	2	8		5	92	
Ba^{2+}-APS	112	3	2		8	5		
BAPTA-AM-APS	112	3	2		8	5		0.05

All solutions were at pH 7.2. NA-APS was APS + 300 μM niflumic acid.

Table 2

Intracellular solutions

	K-gluconate	NaCl	HEPES	$CaCl_2$	$MgCl_2$	K-BAPTA	Adenosine triphosphatase	Guanosine triphosphate
Intracellular solution (perforated patch)	90	10	10	2	2			
Intracellular solution (whole-cell patch)	90	10	10	0.023	2	5	3	0.6

All solutions were at pH 7.2.